

# Assessing the Impact of Vaccination on COVID-19 in South Africa Using Mathematical Modeling

Musyoka Kinyili\*, Justin B. Munyakazi and Abdulaziz Y. A. Mukhtar

Department of Mathematics and Applied Mathematics, Faculty of Natural Sciences, University of the Western Cape, Private Bag X17, Bellville 7535, South Africa

Received: 12 Aug. 2021, Revised: 14 Sep. 2021, Accepted: 26 Sep. 2021

Published online: 1 Nov. 2021

**Abstract:** The unexpected continuing mushrooming tendency of the COVID-19 epidemic calls for alarm in the entire globe especially with the cropping up of more divergent contagious variants being witnessed. On top of the many non-pharmaceutical measures put in place for containment of the pandemic, pharmacological measures have been incorporated in the battle against the SARS-CoV-2 especially with the commencement of vaccination in the early December 2020. This study develops a deterministic compartmental model that incorporates vaccination as a measure to combat the spread of COVID-19 epidemic. We use the model particularly to assess the potential impact of vaccination in shattering the chain of transmission of the virus in South Africa. Verification of the model is carried out by performing its best fit to cumulative COVID-19 positive cases data as reported by the government of the Republic of South Africa utilizing the maximum likelihood estimation algorithm implemented in fitR package. With some vaccines already being under utility while other are being developed, we consider two major vaccine efficacy scenarios. One scenario accounts for general hypothetical vaccines with 20%, 50%, 65% and 85% case efficacy. The other scenario considers the Johnson and Johnson's Janssen vaccine with its distinctive efficacy levels as reported to act against the 501Y.V2 variant. The sensitivity analysis and simulations for the model reveal that the cumulative infections decline drastically with increased extent of vaccination at each level of the vaccine efficacy. The study fundamentally discovers that vaccinating approximately 20% of the population with a vaccine of at least 60% efficacy would be sufficient in elimination of the pandemic over relatively shorter time. Moreover, with J&J vaccine maintaining its efficacious level against the 501Y.V2 variant, it would be the best vaccine to shortly eradicate the COVID-19 epidemic in South Africa.

**Keywords:** Control measures; COVID-19; COVID-19 vaccination; Mathematical modeling; Vaccine efficacy; Simulations.

## 1 Introduction

Severe Acute Respiratory Syndrome-Corona-virus-2 (SARS-CoV-2) the agent initiator of the COVID-19 pandemic [1,2,3,4] has never been experienced before in the human geographical setting [5]. Since its first report in the late December 2019 in Wuhan China [3,6,7,8], the world has been seriously battling with the epidemic confirming that the pandemic has been one of the greatly taxing global health emergencies in the modern history [9]. By June 3, 2021, over 172 million COVID-19 associated cumulative infections with more than 3.7 million fatalities have been confirmed in the whole world. Strangely, the disease has been presenting itself in wave after wave as observed in many countries globally probably due to the mutational characteristic of the causative agent. This tendency of the virus has remarkably contributed to its long-unexpected delayed

clearance from the human host. This fact makes the pandemic to keep on being deep-rooted and sustainable mushrooming in many global regions.

Many non-pharmaceutical measures put in place world-wide have significantly been of aid in containing the spread of the virus [10]. Rigorous scientific research has also been conducted since early 2020 with more than 50 companies joining in to develop anti-COVID-19 vaccines [11]. Based on the history of deadly diseases encountered in humans before, pharmacological measures serve better in prevention and eradication of such diseases. In line with this fact, there has been campaigns for adoption of the approved COVID-19 vaccines available. Some of these vaccines include Pfizer-BioNTech, Moderna, Oxford-AstraZeneca and Johnson and Johnson's Janssen (J&J) [11,12]. These vaccines have received authorization for emergency use by regulatory bodies in various countries [12]. Some of

\* Corresponding author e-mail: [4100150@myuwc.ac.za](mailto:4100150@myuwc.ac.za)

these regulatory bodies are the UK Medicine and Health Products Regulatory Agency (MHRA), US Food and Drug Administration (FDA) and Europe Medicine Agency (EMA) [13].

Pfizer-BioNTech vaccine was firstly approved for use in UK on December 2, 2020 with the Oxford-AstraZeneca and Moderna vaccines being approved on December 20, 2020 and January 8, 2021 respectively [11]. Evaluation of mass vaccination campaigns and clinical trials have established that Pfizer-BioNTech, Oxford-AstraZeneca and Moderna vaccines can provide high levels of protection against COVID-19 moderate to severe symptomatic conditions especially with 2 shots administered after 3 to 4 weeks apart [14, 15, 16, 17]. However, vaccines delivery has been taxing due to the supply inadequacy and restricted capacity of distribution in most countries world-wide led by developing countries [12]. About 92 low- and middle-income countries are procuring the COVID-19 vaccines via the COVAX Advance Market Commitment (AMC) Facility which is a world-wide risk-sharing mechanism for the collaborative procurement of the COVID-19 vaccines [18]. The countries reinforced by the COVAX Facility are scheduled to pay for the procured vaccines once they have been licensed by the World Health Organization (WHO). These countries are encouraged to vaccinate the fore-line health care worker in the first priority. The COVAX Facility further aims to provide vaccines for vaccinating about 20% of the countries' population especially those at high risk.

The single-dose J&J vaccine was firstly rolled out on February 18, 2021 in the Republic of South Africa. This was based on the reason that the vaccine was found to work better against the contagious South African COVID-19 variant (501Y.V2) unlike the Oxford-AstraZeneca vaccine which had been procured before by the government of the Republic of South Africa [19]. The US Food and Drug Administration (FDA) [20] confirmed previously that J&J vaccine had 57% efficacy against the more contagious 501Y.V2 variant. Amazingly, their further clinical trials re-confirmed that the vaccine was 64% efficacious, it could offer 73% protection against moderate to severe COVID-19 infections 14 days after vaccination and could offer 82% protection 28 days after receiving the dose. This report was posted online by US FDA on February 24, 2021. As of April 24, 2021, the Republic of South Africa had vaccinated about 479,768 people with J&J vaccine [19]. These were majorly the front-line health care workers which were prioritized to be vaccinated in phase 1 of the Sisonke vaccination program. This accounts for approximately 1% of the Republic of South Africa total population [19].

COVID-19 has continuously animated the scientific research arena with more insight being drawn to the understanding of its transmission dynamics and control measures in prolific effort to diminish the epidemic. To achieve such, scientists have greatly used mathematical modeling tool with extension of the SIR and SEIR

compartmental mathematical models [21, 22, 23, 24, 25, 26, 27]. Inference by [28] heed that mathematical modeling is a utility tool for provision of realistic discernment into the transmission dynamics and containment of escalating infectious disease such as COVID-19. Moreover, [29, 30] report that mathematical modeling technique has a long tract record of utilization as a tool used to examine policy. It is recently being adapted extensively to study the dynamics of the COVID-19 epidemic especially modeling of anti-COVID-19 vaccines' impacts and administration strategies as adopted in different countries in the entire globe.

For instance, in [31], modified SEIR compartmental model is used to assess the impact of an hypothetical imperfect anti-COVID-19 vaccine on the control of the pandemic. They derived an analytical expression for the minimum percentage of un-vaccinated susceptible individuals who needed to be vaccinated in order to achieve-induced community herd immunity. In [18], a mathematical model which aimed at simulating different vaccine allocation strategies in India is developed. The model is used to assess these vaccine allocation strategies while varying potential vaccine characteristics. Further, an evaluation of the relative COVID-19 cases and deaths under varying control measures is considered. In [29], mathematical modeling is employed to examine the possible outcomes of different vaccination scenarios. The distinction between projection against infections, onward transmission and disease, and differential protection effects on the elderly is considered. In [13], a compartmental mathematical model is developed and used to study the COVID-19 transmission dynamics with mass vaccination strategy. Social distancing and testing against the COVID-19 pandemic as part of containing its spread is also factored in. In [12], a mathematical model incorporating evaluation of the COVID-19 vaccination strategies with delayed second dose administration is done. In [11], an existing age-structured and regionally-structured mathematical model of SARS-CoV-2 dynamics matched to UK data is adapted. The model is further used to study vaccination and non-pharmaceutical interventions against the spread of the COVID-19 epidemic.

In this belt, this study seeks to develop a deterministic compartmental mathematical model incorporating an anti-COVID-19 vaccine in significant contribution to battle the COVID-19 epidemic. We use the model specifically to assess the potential impact of vaccination in shattering the chain of transmission of the SARS-CoV-2 in South Africa. The remaining part of the paper is structured as follows: We devote Section 2 to model formulation. In Section 3, we analyze the model properties proving positivity and boundedness, local and global stability of disease free equilibrium. In Section 4, we present results analysis and discussion including model validation, sensitivity analysis, and numerical simulations. Finally, in Section 5 we give the conclusion.

## 2 Model Formulation

We give the descriptive formulation of the hereby proposed compartmental deterministic model incorporating vaccination against the COVID-19 pandemic. We subdivide the cumulative human population  $N(t)$  into six discordant classes specifically the susceptible class ( $S(t)$ ), the susceptible-vaccinated class ( $S_V(t)$ ), the latent class ( $E(t)$ ), the infectious class of individuals who are symptomatic ( $I_s(t)$ ), the infectious class of individuals who are asymptomatic ( $I_A(t)$ ) and the class of individuals who are removed from the chain of transmission of the disease ( $R(t)$ ). Therefore, the total human population over time  $t$  for the proposed model is

$$N(t) = S(t) + S_V(t) + E(t) + I_s(t) + I_A(t) + R(t). \quad (1)$$

The flow diagram for the proposed model is depicted by Figure 1. The model assumes that the vaccinated individuals can be removed from the disease’s transmission cycle following their highly boosted immunity and their wise choices of continuing to adhere to the containment protocols put in place. The resultant model system of ordinary differential equations is

$$\frac{dS}{dt} = \pi - (\gamma + \omega + \mu)S \quad (2)$$

$$\frac{dS_V}{dt} = \omega S - ((1 - \alpha)\Lambda\gamma + \alpha\Lambda + \mu)S_V \quad (3)$$

$$\frac{dE}{dt} = \gamma S + (1 - \alpha)\Lambda\gamma S_V - (\eta + \mu)E \quad (4)$$

$$\frac{dI_s}{dt} = \rho\eta E - (\phi + \mu)I_s \quad (5)$$

$$\frac{dI_A}{dt} = (1 - \rho)\eta E - (\psi + \mu)I_A \quad (6)$$

$$\frac{dR}{dt} = \alpha\Lambda S_V + \phi I_s + \psi I_A - \mu R \quad (7)$$

where

$$\gamma = \beta(\xi I_s + I_A) \quad (8)$$

is the force of infection with  $\xi < 1$  being the modification parameter since generally the asymptomatic individuals are assumed to be more infectious than the symptomatic individuals. The other model parameters are defined in Table 1.

## 3 Model Properties

We point out that the model describes human population, and therefore it is very key to analyze the model’s properties in preservation of the epidemiological meaningfulness [32]. Due to this paramount reason, we present the analysis of the model (2) - (7) basic features.

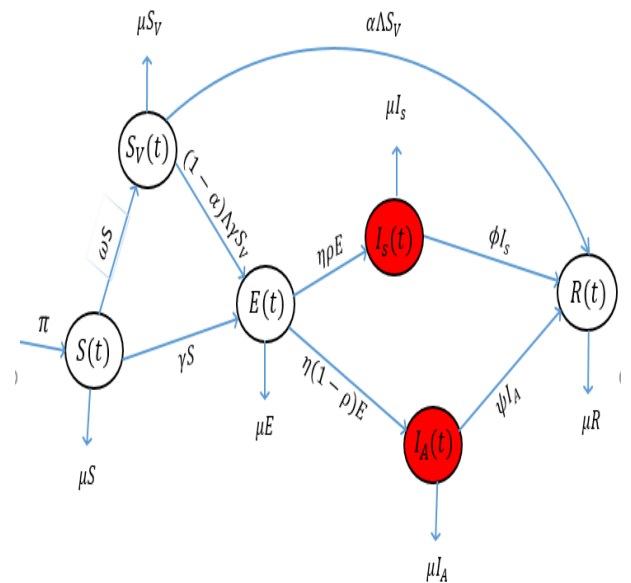


Fig. 1: The proposed model assimilating vaccination against COVID-19.

### 3.1 Positivity of the Solution

We demonstrate that the model’s solution prevail positive for all  $t \geq 0$ . We state and prove a Lemma as follows

**Lemma 3.1**

Let  $S(0) \geq 0, S_V(0) \geq 0, E(0) \geq 0, I_s(0) \geq 0, I_A(0) \geq 0$  and  $R(0) \geq 0$ . Then the solution  $S(t) > 0, S_V(t) > 0, E(t) > 0, I_s(t) > 0, I_A(t) > 0$  and  $R(t) > 0$  exist  $\forall t \geq 0$ .

**Proof**

Suppose that the solution of the model (2) - (7) is not positive for all  $t \geq 0$ . Then there exist a first time  $t^* > 0$  such that

$$t^* = \inf\{t \mid S(t) = 0 \text{ or } S_V(t) = 0 \text{ or } E(t) = 0 \text{ or } I_s(t) = 0 \text{ or } I_A(t) = 0 \text{ or } R(t) = 0\}.$$

If  $S(t^*) = 0$ , then  $\forall t \in (0, t^*), S(t) > 0, S_V(t) > 0, E(t) > 0, I_s(t) > 0, I_A(t) > 0$  and  $R(t) > 0, \frac{dS(t^*)}{dt} < 0$ .

However, from (2)  $\frac{dS(t^*)}{dt} = \pi > 0$  (since all the model parameters are defined to be positive). This contradicts the initial assumption that  $\frac{dS(t^*)}{dt} < 0$ . Hence  $S(t) > 0$  for all  $t \geq 0$ . Adapting similar argument, it can be proved that  $S_V(t), E(t), I_s(t), I_A(t)$  and  $R(t)$  are positive for all  $t \geq 0$ .

### 3.2 The Invariant Region

We next ascertain that the model’s solution is bounded and hold out in the positive region for all  $t \geq 0$ . This is accomplished by proving that the biological feasible region predefined here as

$$\mathcal{D}_R = \left\{ (S, S_V, E, I_s, I_A, R) \in \mathbb{R}_+^6 : S + S_V + E + I_s + I_A + R \leq \frac{\pi}{\mu} \right\} \quad (9)$$

is positively invariant with respect to the model (2) - (7).

**Table 1:** Parameter description for the model (2) - (7) and their estimated values.

Symbol	Parameter Description	Value per day	Source
$\pi$	Recruitment rate	11244	[5]
$\beta$	Effective contact rate	1.0598	[5]
$\omega$	Measure of vaccination	(0,1)	Variable
$\alpha$	Measure of vaccine efficacy	(0,1)	Variable
$\alpha\Lambda$ ((1 - $\alpha$ ) $\Lambda$ )	Rate at which susceptible-vaccinated individuals are removed (become latent)	$\Lambda = 0.9$	Fitted
$\rho\eta$ ((1 - $\rho$ ) $\eta$ )	Symptomatic (asymptomatic) development by the latent individuals	$\rho = 0.27$ $\eta = 0.1961$	Fitted [13,18]
$\xi$	Infectious rate by the symptomatic individuals	0.3214	[31]
$\phi$	Removal rate by the symptomatic individuals	0.1429	[31]
$\psi$	Removal rate by the asymptomatic individuals	0.3115	Fitted
$\mu$	Natural death rate	0.0001	Fitted

Noticing that

$$\frac{dN}{dt} = \pi - \mu N. \quad (10)$$

We obtain

$$N(t) = \frac{\pi}{\mu} (1 - e^{-\mu t}) + N_0 e^{-\mu t}, \quad (11)$$

where  $N_0 = N(0)$ .

Using comparison theorems on ODEs (11) (see [33]) yields

$$\lim_{t \rightarrow \infty} N(t) \leq \frac{\pi}{\mu}. \quad (12)$$

Equation (12) hints that  $N \leq \frac{\pi}{\mu}, \forall t \geq 0$ . We deduce that  $N$  is bounded thus culminating that the feasible region  $\mathcal{D}_{\mathcal{R}}$  is positively invariant and attracting. Hence it is in order to consider the dynamics of the model (2) - (7) in  $\mathcal{D}_{\mathcal{R}}$  for all  $t \geq 0$ . The model can now be considered as epidemiologically and mathematically well posed in the  $\mathcal{D}_{\mathcal{R}}$  [34].

### 3.3 The Model Stability Analysis

We establish that the proposed model has a unique disease free equilibrium (DFE)  $\mathcal{E}^*$  with

$$\mathcal{E}^* = (S^*, S_V^*, 0, 0, 0, R^*) \quad (13)$$

where

$$\begin{aligned} S^* &= \frac{\pi}{\omega + \mu}, \\ S_V^* &= \frac{\pi \omega}{(\omega + \mu)(\alpha \Lambda + \mu)}, \\ R^* &= \frac{\alpha \Lambda \pi \omega}{\mu(\omega + \mu)(\alpha \Lambda + \mu)}. \end{aligned} \quad (14)$$

#### 3.3.1 The Disease Free Equilibrium Local Stability

We compute the basic reproduction number of the model in order to analyze the local stability of the DFE. It represents the average secondary number of infections that result from one infected individual when introduced in a totally susceptible population. We denote the basic reproduction by  $\mathcal{R}_0$  and adopt the next generation matrix (NGM) technique for its computation [32].

From the model (2) - (7) the Jacobian for secondary infections  $F$  and transfer of infections  $V$  are respectively given by

$$F = \begin{pmatrix} 0 & \frac{\beta \xi \pi}{(\omega + \mu)} \left(1 + \frac{(1 - \alpha)\omega \Lambda}{\alpha \Lambda + \mu}\right) & \frac{\beta \pi}{(\omega + \mu)} \left(1 + \frac{(1 - \alpha)\omega \Lambda}{\alpha \Lambda + \mu}\right) \\ 0 & 0 & 0 \\ 0 & 0 & 0 \end{pmatrix}, \quad (15)$$

and

$$V = \begin{pmatrix} \eta + \mu & 0 & 0 \\ -\rho \eta & \phi + \mu & 0 \\ -(1 - \rho)\eta & 0 & \psi + \mu \end{pmatrix}, \quad (16)$$

$$FV^{-1} = \begin{pmatrix} \frac{\beta \pi}{(\omega + \mu)(\eta + \mu)} \ell \left\{ \frac{\rho \eta \xi}{\phi + \psi} + \frac{(1 - \rho)\eta}{\psi + \mu} \right\} & \frac{\beta \pi \xi}{(\omega + \mu)(\phi + \mu)} \ell & \frac{\beta \pi}{(\omega + \mu)(\psi + \mu)} \ell \\ 0 & 0 & 0 \\ 0 & 0 & 0 \end{pmatrix} \quad (17)$$

where

$$\ell = 1 + \frac{(1 - \alpha)\omega\Lambda}{\alpha\Lambda + \mu}. \tag{18}$$

Hence the basic reproduction number for the model is

$$\mathcal{R}_0 = \frac{\beta\pi}{(\omega + \mu)(\eta + \mu)} \ell \left\{ \frac{\xi\rho\eta}{\phi + \psi} + \frac{(1 - \rho)\eta}{\psi + \mu} \right\}. \tag{19}$$

The DFE of the model is locally asymptotically stable if  $\mathcal{R}_0 < 1$ . The basic reproduction number  $\mathcal{R}_0$  displays the contributions of the symptomatic and the asymptomatic individuals to the infections and can be written as  $\mathcal{R}_0 = \mathcal{R}_{0s} + \mathcal{R}_{0A}$  where

$$\mathcal{R}_{0s} = \frac{\beta\pi}{(\omega + \mu)(\eta + \mu)} \ell \left\{ \frac{\xi\rho\eta}{\phi + \psi} \right\} \quad \text{and}$$

$$\mathcal{R}_{0A} = \frac{\beta\pi}{(\omega + \mu)(\eta + \mu)} \ell \left\{ \frac{(1 - \rho)\eta}{\psi + \mu} \right\}.$$

### 3.3.2 The Disease Free Equilibrium Global Stability

We verify the model's DFE global stability employing the approach used by [35]. We state and prove a Lemma in this case.

**Lemma 3.3.2**

Let the model be expressible in the form,  $\frac{d\mathbf{X}}{dt} = F(\mathbf{X}, \mathbf{Y})$ ,  $\frac{d\mathbf{Y}}{dt} = G(\mathbf{X}, \mathbf{Y})$ ,  $G(\mathbf{X}, 0) = 0$ , where vector  $\mathbf{X}$  represents the uninfected classes and vector  $\mathbf{Y}$  is the disease classes of the model. The fixed point  $\mathcal{E}^* = (\mathbf{X}^*, 0)$  for the model is globally asymptotically stable (g. a. s) if and only if  $\mathcal{R}_0 < 1$  and the following conditions are satisfied

- $C_1 : \frac{d\mathbf{X}}{dt} = F(\mathbf{X}, 0)$ ,  $\mathbf{X}^*$  is globally asymptotically stable.
- $C_2 : G(\mathbf{X}, \mathbf{Y}) = Z\mathbf{Y} - \tilde{G}(\mathbf{X}, \mathbf{Y})$ ,  $\tilde{G}(\mathbf{X}, \mathbf{Y}) \geq 0$  for  $(\mathbf{X}, \mathbf{Y}) \in \mathbb{R}_+^6$  where  $Z = \frac{\partial G}{\partial \mathbf{Y}} \mathcal{E}^*$  and  $\mathbb{R}_+^6$  is the region where the model makes biological sense.

**Proof**

From the model system (2) - (7), we heed that  $\mathbf{X} = (S, S_V, R)^T$  and  $\mathbf{Y} = (E, I_s, I_A)^T$ . The model's DFE is  $\mathcal{E}^* = (\mathbf{X}^*, 0)$  as set up by (13). The point  $\mathcal{E}^* = (\mathbf{X}^*, 0)$  is g. a. s if  $\mathcal{R}_0 < 1$ , thus

$$\frac{d\mathbf{X}}{dt} = F(\mathbf{X}, 0) = \begin{bmatrix} \pi - (\omega + \mu)S \\ \omega S - (\alpha\Lambda + \mu)S_V \\ \alpha\Lambda S_V - \mu R \\ 0 \end{bmatrix} \quad \text{hence the}$$

condition  $C_1$  is plainly satisfied. For condition  $C_2$

$$ZY = \begin{pmatrix} -(\eta + \mu) & 0 & 0 \\ \rho\eta & -(\phi + \mu) & 0 \\ (1 - \rho)\eta & 0 & -(\psi + \mu) \end{pmatrix} \begin{pmatrix} E \\ I_s \\ I_A \end{pmatrix} \tag{20}$$

and

$$G(\mathbf{X}, \mathbf{Y}) = \begin{pmatrix} \beta(\xi I_s + I_A)S + (1 - \alpha)\beta(\xi I_s + I_A)S_V \\ \rho\eta E - (\phi + \mu)I_s \\ (1 - \rho)\eta E - (\psi + \mu)I_A \end{pmatrix}. \tag{21}$$

From the identity that  $G(\mathbf{X}, \mathbf{Y}) = Z\mathbf{Y} - \tilde{G}(\mathbf{X}, \mathbf{Y})$ , then it indicates that

$$\tilde{G}(\mathbf{X}, \mathbf{Y}) = \begin{pmatrix} \beta(\xi I_s + I_A)(1 - \frac{S}{N}) + (1 - \alpha)\beta(\xi I_s + I_A)(1 - \frac{S_V}{N}) \\ 0 \\ 0 \end{pmatrix}. \tag{22}$$

We note that since  $0 \leq S_V \leq S \leq N$ , then  $\tilde{G}(\mathbf{X}, \mathbf{Y}) \geq 0$  hence condition  $C_2$  is satisfied. Thus we conclude that the DFE of the model is globally asymptotically stable whenever  $\mathcal{R}_0 < 1$ .

## 4 Results Analysis and Discussion

### 4.1 Model Validation

Owing to the fact that fitting of any developed model to real data is a paramount aspect particularly for the authentication of the model's use for scenario testing via numerical simulations, we perform the fitting of the model (2) - (7). The data utilized is the cumulative COVID-19 positive cases as reported by the government of the Republic of South Africa in the period between 10th of June 2020 and 31st of July 2020 [19]. We adopt the Maximum likelihood estimation (MLE) algorithm implemented in fitR package to fit the model to the data. The goodness of fit is depicted by Figure 2.

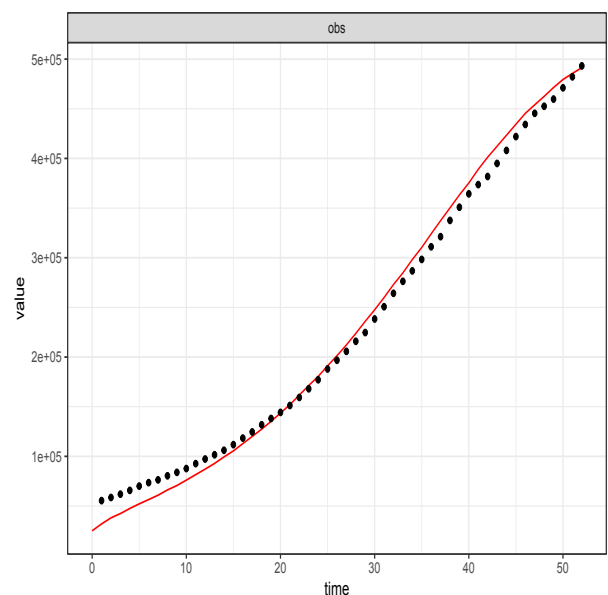


**Fig. 2:** The model (2) - (7) fit to cumulative COVID-19 positive reported cases (10 June - 31 July 2020) in South Africa. The black-dotted line represents the reported data for COVID-19 positive cases whereas the red-continuous line shows the goodness of fit. Parameter values used are as listed in Table 1 with  $\omega = 0.00001$  and  $\alpha = 0.00001$ .

## 4.2 Sensitivity Analysis

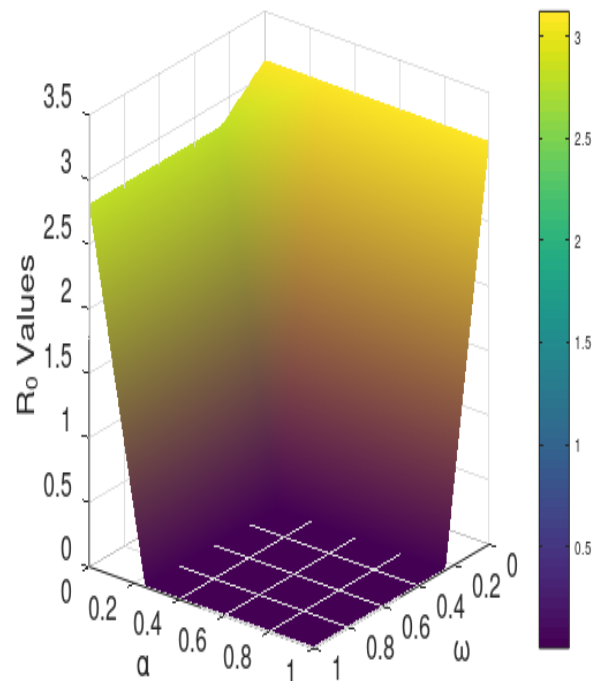
For the purpose of ascertaining the impact(s) of any parameter(s) of research engrossment on the dependent variable, sensitivity analysis is undertaken. The cardinal parameters of regard for this research are  $\omega$  and  $\alpha$  for the measure of vaccination and the vaccine efficacy respectively. We define to have poor vaccination and poor vaccine efficacy if both parameters approach zero whereas perfect vaccination and perfect vaccine efficacy is achieved when both parameters draw closely to unity thus  $0 < \omega < 1$  and  $0 < \alpha < 1$ . We carry out sensitivity analysis for our model to establish the effects of the aforementioned parameters on the basic reproduction number  $\mathcal{R}_0$ . This is done graphically using (19).

Figure 3 illustrates how the basic reproduction number varies with the measure of vaccination  $\omega$  and measure of vaccine efficacy  $\alpha$ . The figure establishes that  $\mathcal{R}_0$  decreases with increase in both the parameters  $\omega$  and  $\alpha$ . Distinctively it obliquely that  $\mathcal{R}_0$  decreases sharply drawing very close to 0 as  $\omega$  and  $\alpha$  assume their extreme values unity (perfect vaccination and vaccine efficacy). This solitary trend fundamentally stipulates that the increased vaccination against COVID-19 using high efficacious vaccine to the general public, would greatly diminish the basic reproduction number and thus stabilizing the DFE to an extent of the pandemic eradication over time.

In addition, considering that the so far approved vaccines for use are currently under very high demand creating scantiness especially in developing countries worldwide and thus delaying the availability of the vaccines, and also the fact that developing a vaccine takes relatively longer time, we consider endorsing a vaccine with a degree of efficacy in bits at varying proportion of vaccination. This is evidenced in Figures 4 and 5. Figure 4 adopts general hypothetical vaccines with different efficacy whereas Figure 5 considers specifically Johnson and Johnson's Janssen vaccine firstly rolled out in South Africa with efficacy as reported by US Food and Drug Administration (see Section 1). Both the figures show how  $\mathcal{R}_0$  values grow small as  $\omega$  advances near its extreme value 1 at rising levels of  $\alpha$ . The figures reveal incredible shift of  $\mathcal{R}_0$  values at different endorsement of vaccine efficacy. A stipulation from these fundamental observations disclose that vaccinating nearly 20% of the population with a vaccine of at least 60% efficacy would suffice to shortly stabilize the disease free equilibrium hence eliminating the COVID-19 pandemic over relatively shorter time.

## 4.3 Numerical Simulations

We carry out numerical simulations using the model principally to test for different scenarios with respect to the parameters of scrutiny for this research work. As aforementioned, the principal parameters of interest here



**Fig. 3:** Variation of the basic reproduction number with  $\omega$  (measure/ extent of vaccination) and  $\alpha$  (measure of vaccine efficacy). Parameter values used are listed in Table 1.

for the proposed model are  $\omega$  denoting the extent of vaccination to the general public and  $\alpha$  for the measure of vaccine efficacy. We simulate all the six classes of the model but narrow down our attention to the symptomatic and asymptomatic infectious classes which abundantly add up to the cumulative infections for COVID-19 epidemic as reported. We consider two major sets of vaccine efficacy scenarios namely the general hypothetical vaccine efficacy array of Four levels and a specific vaccine efficacy level scenario for Johnson and Johnson's Janssen (J&J) vaccine as previously reported to act against the South African COVID-19 variant (501Y.V2). Report released on February 24, 2020 by the US Food and Drug Administration indicated that J&J vaccine was 64% efficacious against moderate to severe COVID-19 infections caused by 501Y.V2 variant as opposed to the initial 57% efficacy established during the earlier clinical trials. Furthermore, the report also revealed that the vaccine efficacy against severe COVID-19 cases was 73%, 14 days after vaccination and increased to 82% at least 28 days after vaccination. This solitary trend for J&J vaccine is completely amazing and thus we found it worthwhile to consider in our model numerical simulations.

Figure 6 illustrates the trajectory of all the six classes of the model (2) - (7) at the instant when the measure of

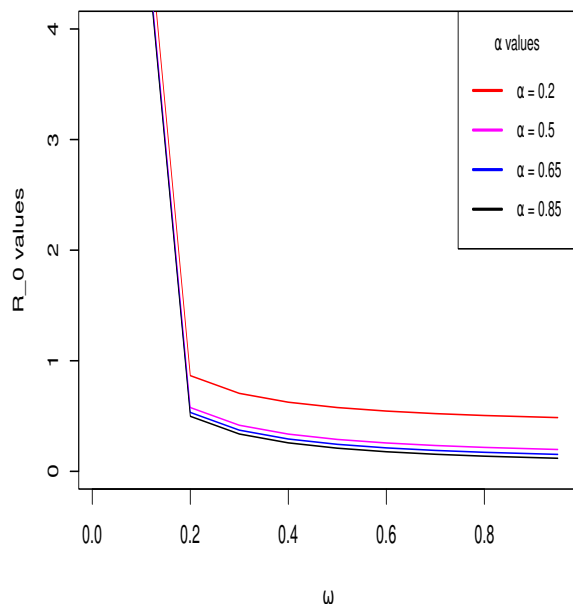


**Fig. 4:** Variation of the basic reproduction number with  $\omega$  (measure of vaccination) at rising levels of vaccine efficacy  $\alpha$  for a general hypothetical vaccine efficacy scenarios. Parameter values used are listed in Table 1.

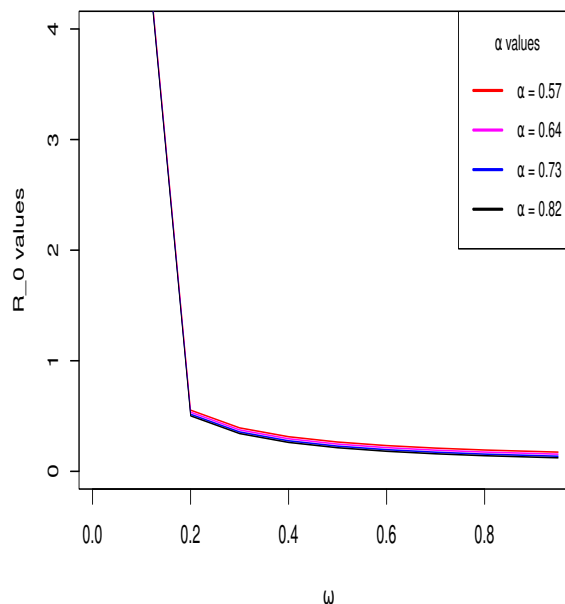


**Fig. 5:** Variation of the basic reproduction number with  $\omega$  (measure of vaccination) at rising levels of vaccine efficacy  $\alpha$  for a specific vaccine efficacy scenarios. Parameter values used are listed in Table 1.

vaccination  $\omega$  and the measure of vaccine efficacy  $\alpha$  levels are extremely minimal. This figure clearly predicts higher plateau numbers of latent cases, symptomatic infectious cases and higher asymptomatic infectious cases summing up to extremely high COVID-19 infections. This trend implies that without the vaccination program, the epidemic would continue escalating hence surging the peak number of the cumulative infections.

Figure 7 demonstrates the trajectory of all the six classes of the model (2) - (7) at the instant when the measure of vaccination  $\omega = 10\%$  and the measure of vaccine efficacy  $\alpha = 60\%$ . This figure depicts very low plateau numbers of latent cases, symptomatic infectious cases as well as low asymptomatic infectious cases resulting in extreme decline in COVID-19 infections. This tendency absolutely divulges that at least 10% of the population vaccinated using a vaccine of 60% efficacy would be very effective reversing the plateau number of COVID-19 epidemic infections. This inference is wholly in concurrence with the solitary threshold observation established by Figures 4 - 5.

#### 4.3.1 General Vaccine Efficacy Scenarios: $\alpha = 20\%$ , $\alpha = 50\%$ , $\alpha = 65\%$ , and $\alpha = 85\%$

For this case, we consider Four levels of vaccine efficacy  $\alpha$  particularly,  $\alpha = 20\%$ ,  $\alpha = 50\%$ ,  $\alpha = 65\%$ , and  $\alpha = 85\%$ . We then simulate the symptomatic and asymptomatic infectious model's classes ( $I_s(t)$  and  $I_A(t)$  respectively) at instances when the extent of vaccination  $\omega$  is 0.01, 0.04, 0.08, 0.12, 0.2, 0.3 (gradually increasing percentages of vaccination). The trajectory tendency for this hypothetical scenario is vividly depicted by Figures 8 – 15. We used the parameter values listed in Table 1. The figures establish accelerated diminishing peak numbers of COVID-19 cumulative infections as the measure of vaccination  $\omega$  increases at each level of individual vaccine efficacy  $\alpha$  scenario. Fundamentally, it is clearly observed that the higher the vaccine efficacy, the lower the percentage of vaccination required to eradicate the epidemic shortly. Uniquely, it is revealed that the plateau number of cumulative infections completely diminish over relatively shorter time when the measure of vaccination is at least 20% with 60% vaccine efficacy.

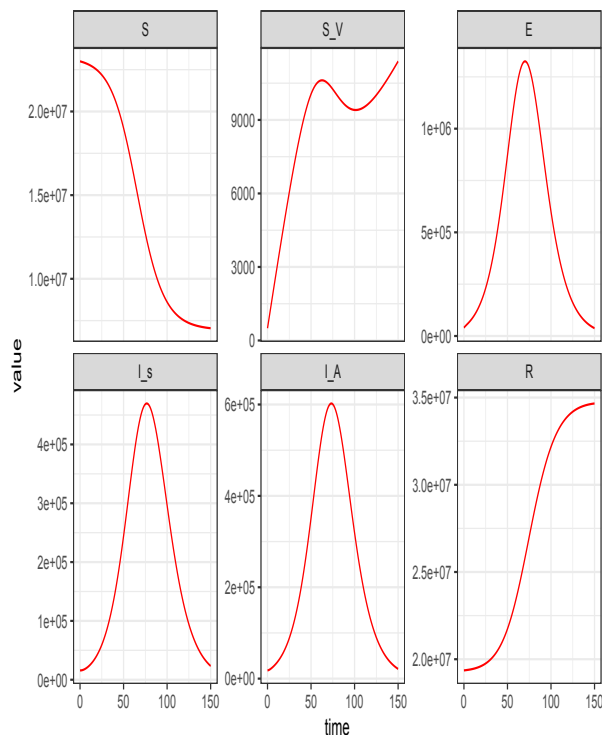


**Fig. 6:** Trajectory simulations of all the six classes of the model (2) - (7) when the measure of vaccination  $\omega$  and the vaccine efficacy  $\alpha$  values are extremely minimal. Parameter values used are listed in Table 1.

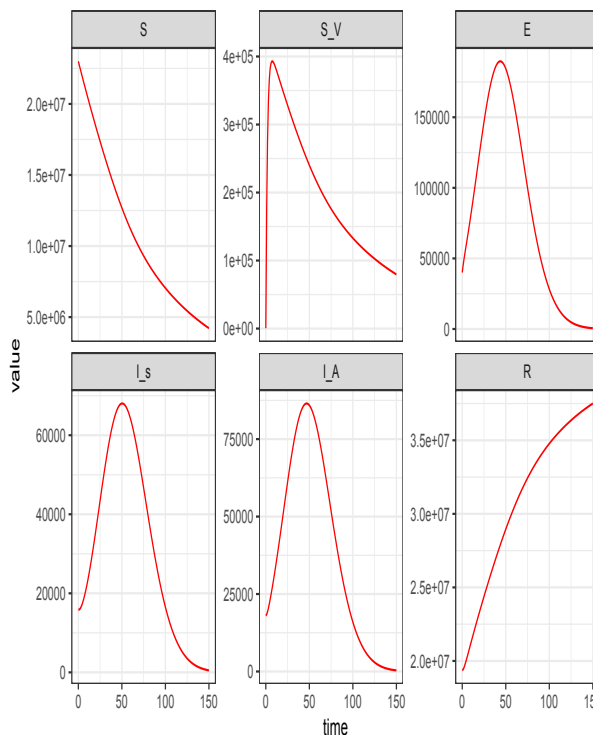


**Fig. 7:** Trajectory simulations of all the six classes of the model (2) - (7) when the measure of vaccination  $\omega = 0.1$  and the vaccine efficacy  $\alpha = 0.6$ . Parameter values used are listed in Table 1.

**4.3.2 Specific Vaccine Efficacy Scenarios:  $\alpha = 57\%$ ,  $\alpha = 64\%$ ,  $\alpha = 73\%$ , and  $\alpha = 82\%$**

For this case, we consider the specific trend efficacy levels for the Johnson and Johnson’s Janssen vaccine as it was reported to act against the South African COVID-19 variant (501Y.V2) (see Section 1). Based on the report, Four levels of J&J vaccine efficacy namely,  $\alpha = 57\%$ ,  $\alpha = 64\%$ ,  $\alpha = 73\%$ , and  $\alpha = 82\%$  are tested. We once again simulate the symptomatic and asymptomatic infectious classes ( $I_s(t)$  and  $I_A(t)$  respectively) of the model at instances when the measure of vaccination  $\omega$  is 0.01, 0.04, 0.08, 0.12, 0.2, 0.3 (gradually increasing percentages of vaccination). The trajectory clear-cut tendency for this specific scenario is illustrated by Figures 16 – 23. We used the parameter values listed in Table 1. The figures depict remarkably accelerated reducing plateau numbers of COVID-19 cumulative infections as the measure of vaccination  $\omega$  increases at each level of the vaccine efficacy. Distinctively, it is plainly observed that J&J vaccine would be the best in shortly eliminating the COVID-19 pandemic in South Africa even when a minimum 12% of the population is vaccinated.

Moreover, as a consequence of remarkable decline in the plateau numbers of both symptomatic and

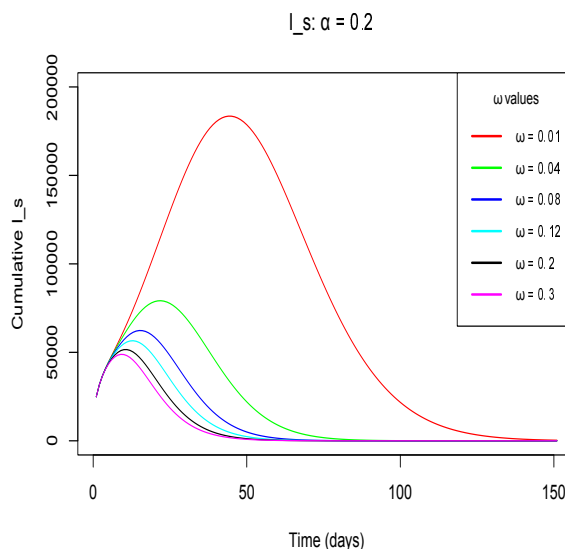


**Fig. 8:** Simulations of the model (2) - (7) showing the cumulative number of  $I_s(t)$  individuals when  $\alpha = 20\%$  as  $\omega$  increases gradually.

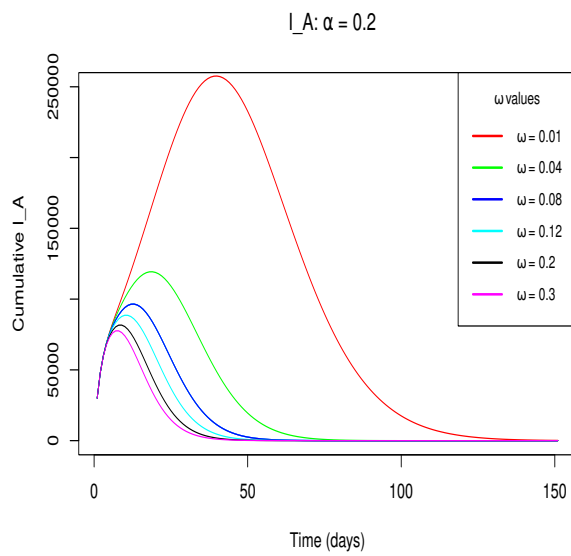


**Fig. 9:** Simulations of the model (2) - (7) showing the cumulative number of  $I_A(t)$  individuals when  $\alpha = 20\%$  as  $\omega$  increases gradually.

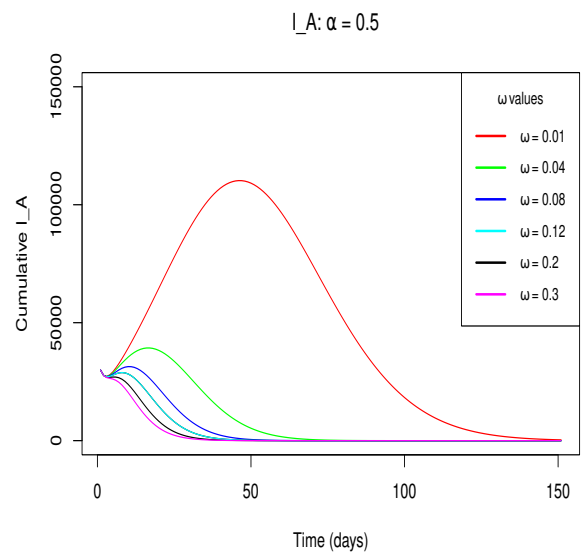


**Fig. 11:** Simulations of the model (2) - (7) showing the cumulative number of  $I_A(t)$  individuals when  $\alpha = 50\%$  as  $\omega$  increases gradually.

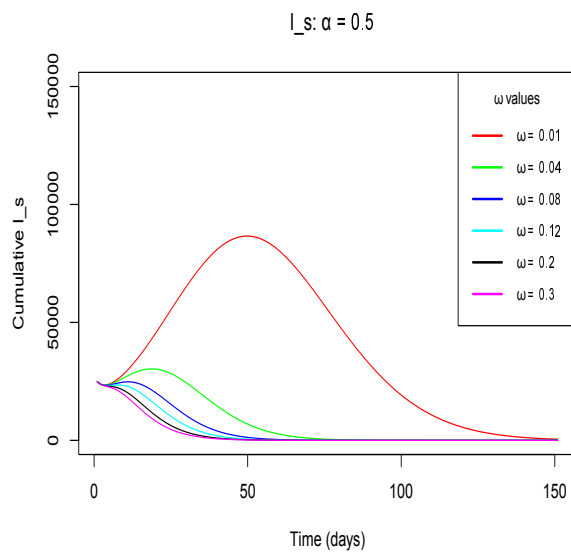


**Fig. 10:** Simulations of the model (2) - (7) showing the cumulative number of  $I_s(t)$  individuals when  $\alpha = 50\%$  as  $\omega$  increases gradually.

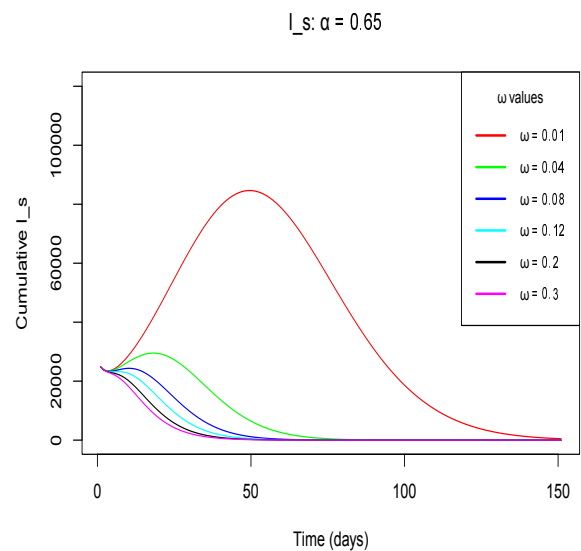


**Fig. 12:** Simulations of the model (2) - (7) showing the cumulative number of  $I_s(t)$  individuals when  $\alpha = 65\%$  as  $\omega$  increases gradually.

asymptomatic cumulative infections, the peak number for the latent individuals keep on diminishing for both the scenarios. This trend is clearly depicted by Figures 24 – 27 for the general hypothetical vaccine efficacy scenario 4.3.1 and Figures 28 – 31 for the specific vaccine efficacy

scenario 4.3.2. This is absolutely in order since as much as the cumulative infections reduce, then the exposures also decrease consequentially.

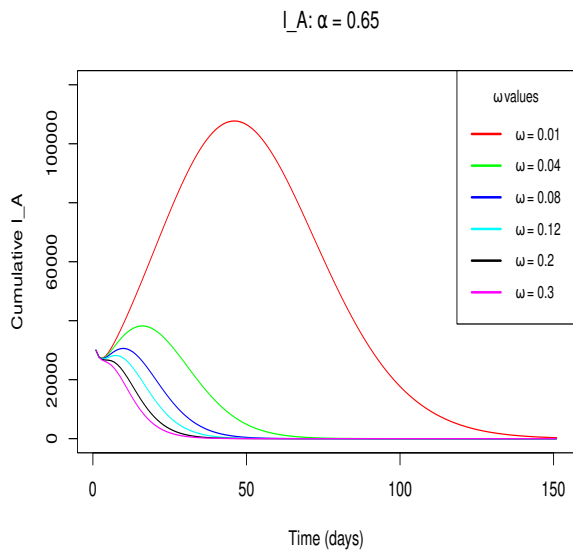


**Fig. 13:** Simulations of the model (2) - (7) showing the cumulative number of  $I_A(t)$  individuals when  $\alpha = 65\%$  as  $\omega$  increases gradually.

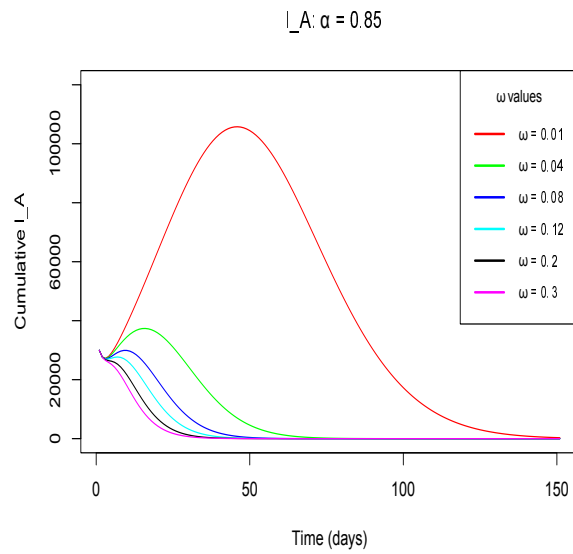


**Fig. 15:** Simulations of the model (2) - (7) showing the cumulative number of  $I_A(t)$  individuals when  $\alpha = 85\%$  as  $\omega$  increases gradually.

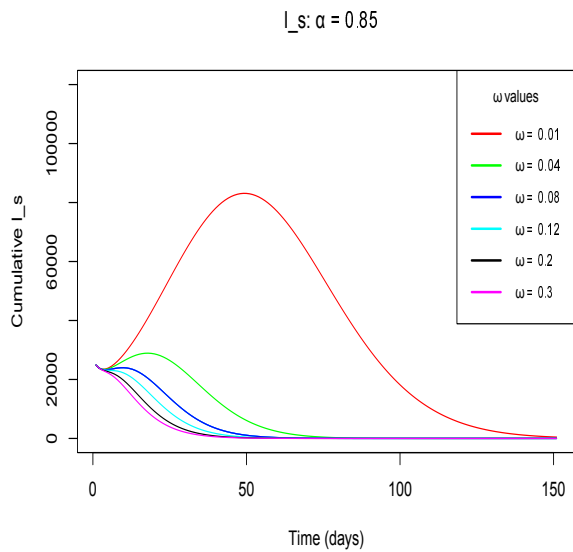


**Fig. 14:** Simulations of the model (2) - (7) showing the cumulative number of  $I_s(t)$  individuals when  $\alpha = 85\%$  as  $\omega$  increases gradually.

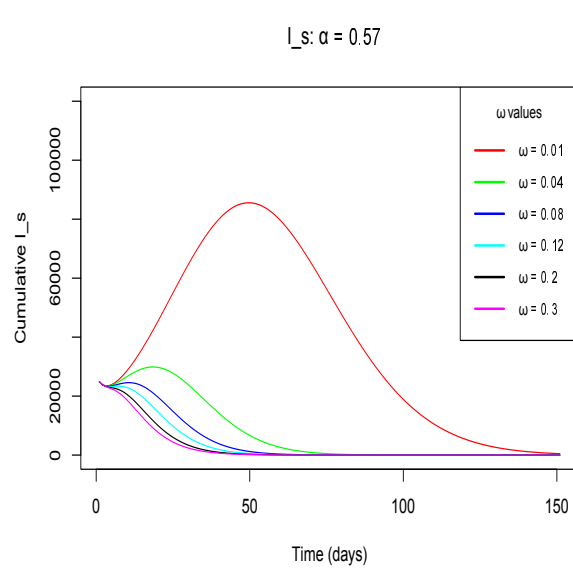


**Fig. 16:** Simulations of the model (2) - (7) showing the cumulative number of  $I_s(t)$  individuals when  $\alpha = 57\%$  as  $\omega$  increases gradually.

## 5 Conclusion

In this work, we formulated a modified SEIR deterministic model. The model's key unique feature was the incorporation of anti-COVID-19 vaccine with some

degree of efficacy. The model's paramount properties were verified to preserve the epidemiological meaningfulness since the model monitored human population. This important exercise ascertained that the

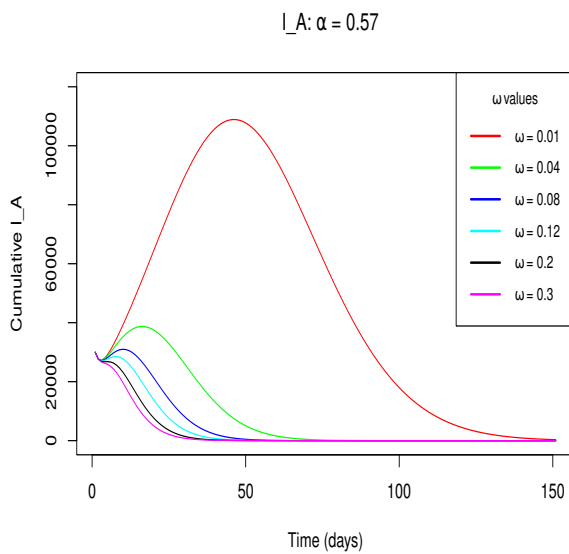


**Fig. 17:** Simulations of the model (2) - (7) showing the cumulative number of  $I_A(t)$  individuals when  $\alpha = 57\%$  as  $\omega$  increases gradually.

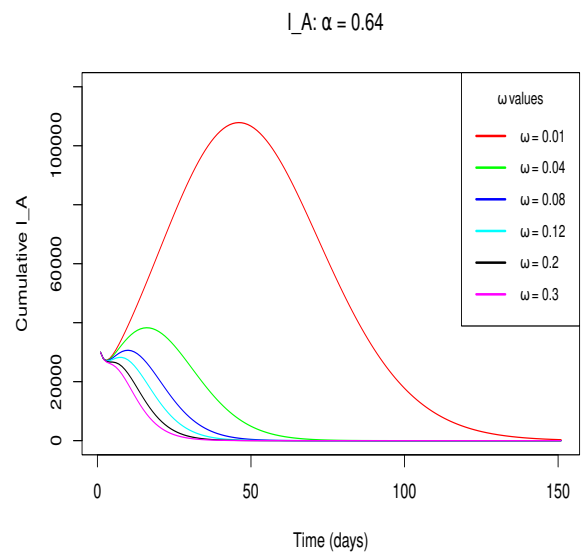


**Fig. 19:** Simulations of the model (2) - (7) showing the cumulative number of  $I_A(t)$  individuals when  $\alpha = 64\%$  as  $\omega$  increases gradually.

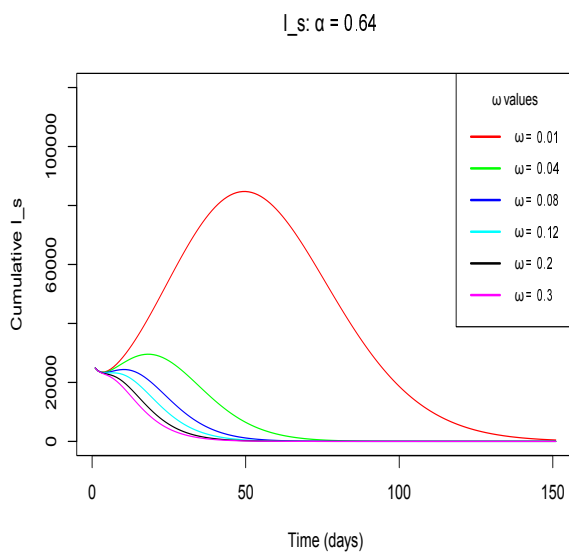


**Fig. 18:** Simulations of the model (2) - (7) showing the cumulative number of  $I_s(t)$  individuals when  $\alpha = 64\%$  as  $\omega$  increases gradually.

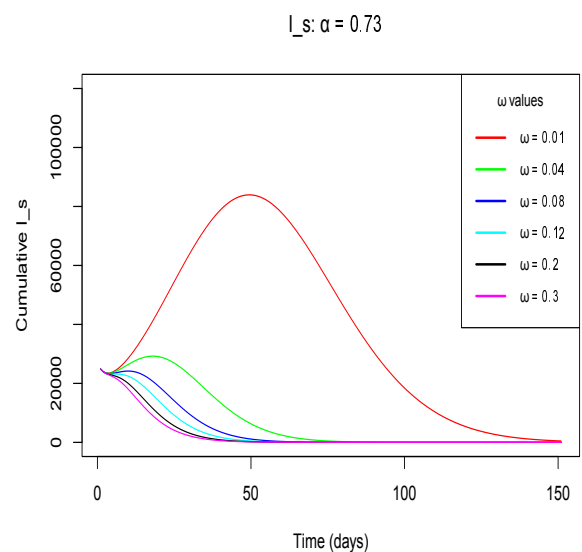


**Fig. 20:** Simulations of the model (2) - (7) showing the cumulative number of  $I_s(t)$  individuals when  $\alpha = 73\%$  as  $\omega$  increases gradually.

solution of the model prevailed positive and bounded for all non-negative time within a defined feasible region.

Additionally, the developed model was validated by carrying out its fitting to COVID-19 positive cases reported data of the Republic of South Africa in the span

from 10th June to 31st July 2020. This authenticated the utility of the model for sensitivity analysis and further simulations. On the account that several vaccines have so far been approved for use while others are still under development and that such vaccines have varying degree

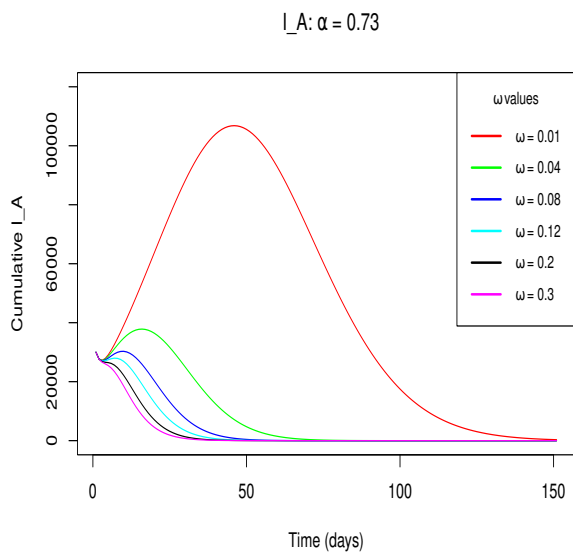


**Fig. 21:** Simulations of the model (2) - (7) showing the cumulative number of  $I_A(t)$  individuals when  $\alpha = 73\%$  as  $\omega$  increases gradually.

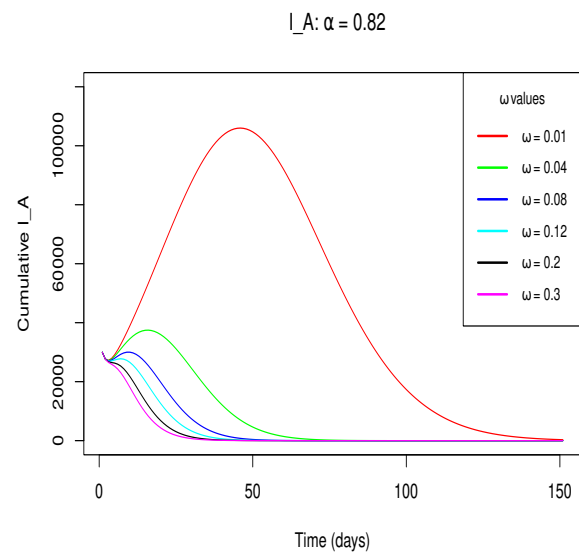


**Fig. 23:** Simulations of the model (2) - (7) showing the cumulative number of  $I_A(t)$  individuals when  $\alpha = 82\%$  as  $\omega$  increases gradually.

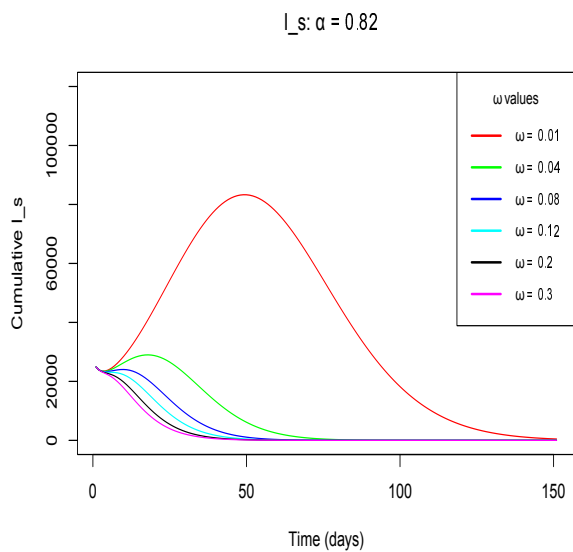


**Fig. 22:** Simulations of the model (2) - (7) showing the cumulative number of  $I_s(t)$  individuals when  $\alpha = 82\%$  as  $\omega$  increases gradually.

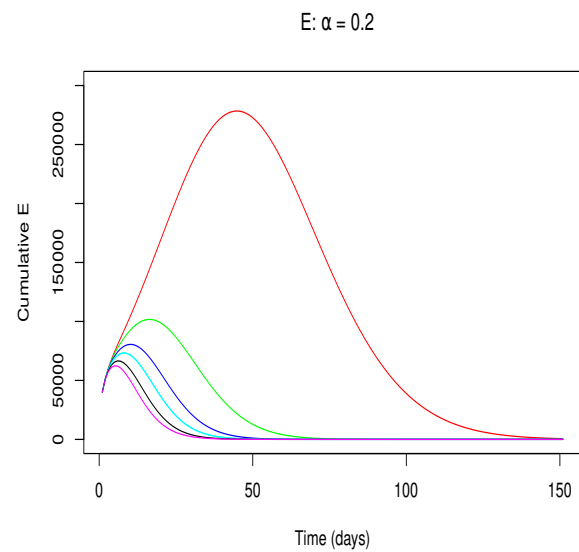


**Fig. 24:** Simulations of the model (2) - (7) showing the cumulative number of  $E(t)$  individuals when  $\alpha = 20\%$  as  $\omega$  increases gradually.

of protection against the COVID-19 pandemic, we considered two major vaccine efficacy scenarios. One scenario accounted for general hypothetical vaccines with 20%, 50%, 65% and 85% case efficacy. The other scenario considered a specific vaccine in particular the Johnson

and Johnson's Janssen vaccine with its distinctive efficacy levels as reported to act against the 501Y.V2 variant by the US Food and Drug Administration.

Sensitivity analysis done for the model depicted that the basic reproduction number decreased with increase in

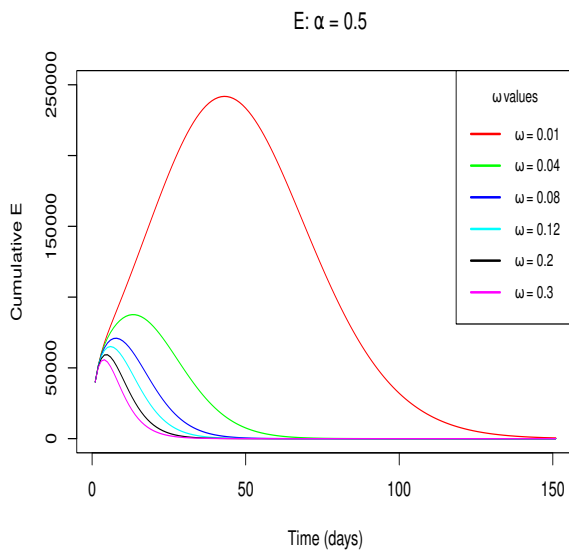


**Fig. 25:** Simulations of the model (2) - (7) showing the cumulative number of  $E(t)$  individuals when  $\alpha = 50\%$  as  $\omega$  increases gradually.

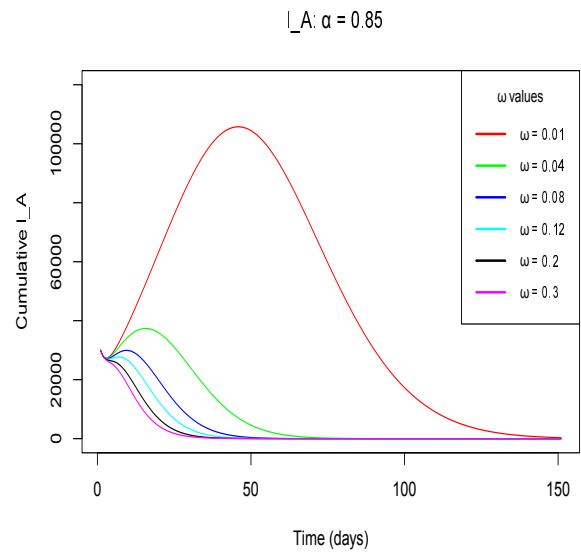


**Fig. 27:** Simulations of the model (2) - (7) showing the cumulative number of  $E(t)$  individuals when  $\alpha = 85\%$  as  $\omega$  increases gradually.

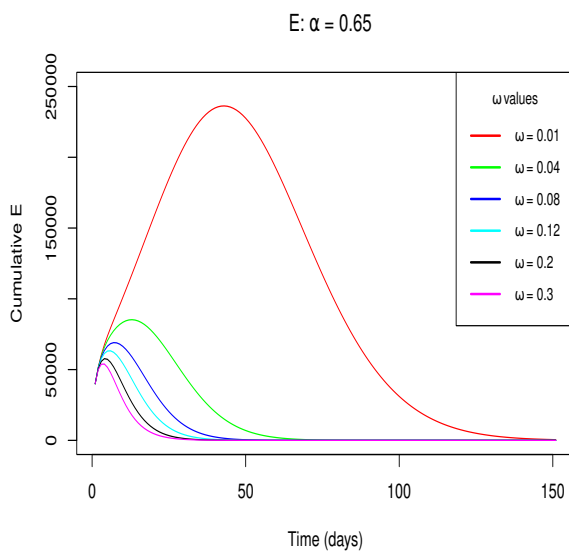


**Fig. 26:** Simulations of the model (2) - (7) showing the cumulative number of  $E(t)$  individuals when  $\alpha = 65\%$  as  $\omega$  increases gradually.

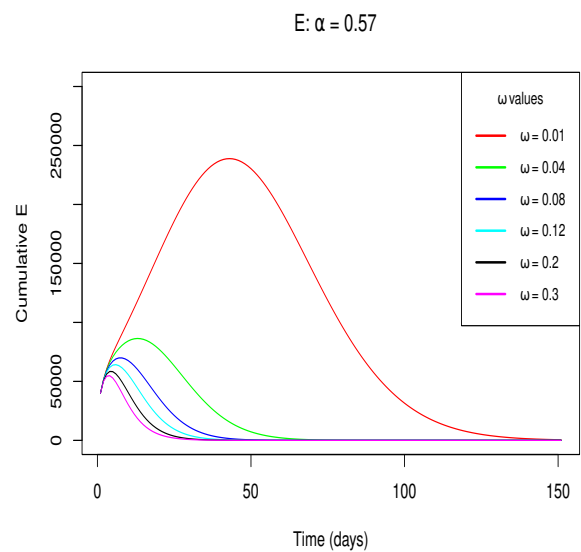


**Fig. 28:** Simulations of the model (2) - (7) showing the cumulative number of  $E(t)$  individuals when  $\alpha = 57\%$  as  $\omega$  increases gradually.

both the extent of vaccination and the vaccine efficacy. It was established that the higher the vaccine efficacy, the lower the percentage of the susceptible population required to be vaccinated in eradication of the epidemic within a shorter span of time.

The model simulations depicted as follows: In absence of anti-COVID-19 vaccination, the model predicted surging peak numbers of both symptomatic and asymptomatic infectious individual amounting to extremely high cumulative infections. The total numbers

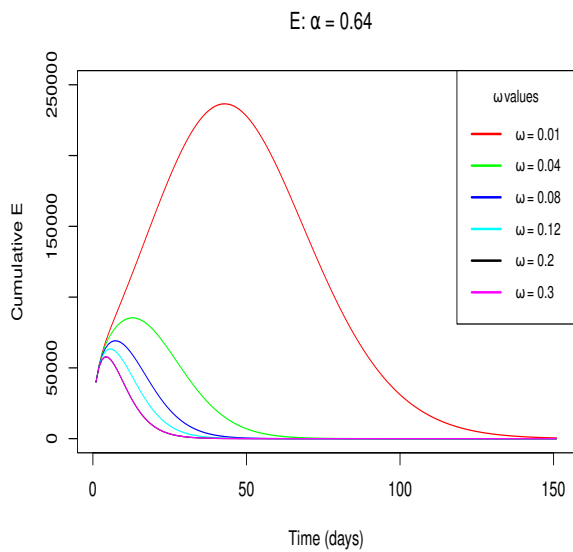


**Fig. 29:** Simulations of the model (2) - (7) showing the cumulative number of  $E(t)$  individuals when  $\alpha = 64\%$  as  $\omega$  increases gradually.

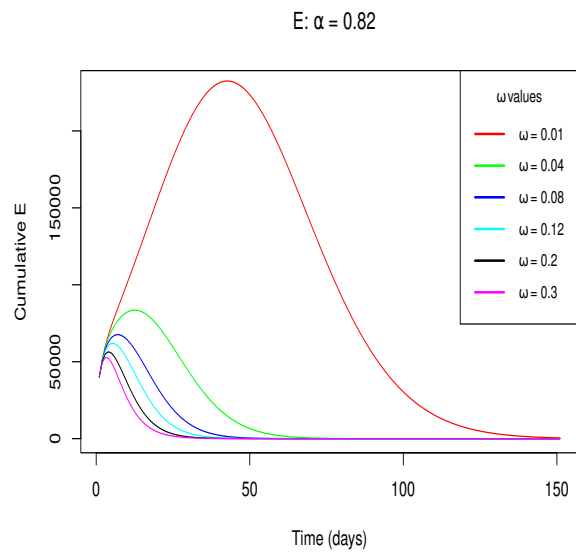


**Fig. 31:** Simulations of the model (2) - (7) showing the cumulative number of  $E(t)$  individuals when  $\alpha = 82\%$  as  $\omega$  increases gradually.

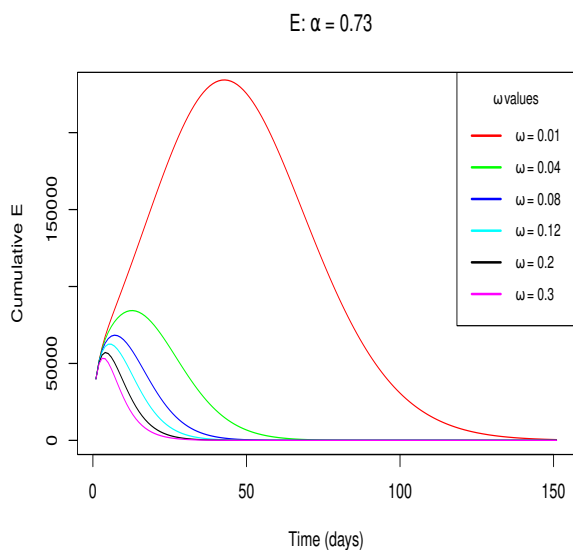


**Fig. 30:** Simulations of the model (2) - (7) showing the cumulative number of  $E(t)$  individuals when  $\alpha = 73\%$  as  $\omega$  increases gradually.

of infections declined drastically at each level of vaccine efficacy as the percentage of vaccination gradually increased for both of the two aforementioned scenarios. This solitary trend consequentially resulted in drastic decline on the cumulative latent cases. In this belt, it was

discovered that vaccinating approximately 20% of the population with a vaccine of at least 60% efficacy would be sufficient in elimination of the pandemic over relatively shorter time. Most remarkably, with J&J vaccine maintaining its efficacious level solitary tendency against the 501Y.V2 variant, it would be the best vaccine to shortly eradicate the COVID-19 epidemic in South Africa. Thus, this study would advocate increased use of the Johnson and Johnson's Janssen vaccine in South Africa as long as it maintain its efficacy level trend.

## Acknowledgments

M. Kinyili acknowledges the **DAAD** German Academic Exchange Service.

J. B. Munyai acknowledges the South African National Research Foundation (NRF).

## Conflict of interest

The authors declare that they have no conflict of interest.

## References

- [1] S. E. Eikenberry, M. Mancuso, E. Iboi, T. Phan, K. Eikenberry, Y. Kuang, E. Kostelich, A. B. Gumel, To mask or not to mask: Modeling the potential for face mask use by the general public to curtail the COVID-19 pandemic, *Infectious Disease Modelling*, 5, 293-308 (2020).

- [2] Z. Mukandavire, F. Nyabadza, N. J. Malunguza, D. F. Cuadros, T. Shiri, and G. Musuka, Quantifying early COVID-19 outbreak transmission in South Africa and exploring vaccine efficacy scenarios, *PLoS One*, 15, e0236003 (2020).
- [3] S. B. Bastos and D. O. Cajueiro, Modeling and forecasting the early evolution of the Covid-19 pandemic in Brazil, *Scientific Reports*, 10, 1-10 (2020).
- [4] A. Ishtiaq, Dynamics of COVID-19 Transmission: Compartmental-based Mathematical Modeling, *Life and Science*, 1, 5 (2020).
- [5] F. Nyabadza, F. Chirove, C. W. Chukwu, and M. V. Visaya, Modelling the potential impact of social distancing on the COVID-19 epidemic in South Africa, *Computational and Mathematical Methods in Medicine*, (2020).
- [6] A. Mollalo, B. Vahedi, and K. M. Rivera, GIS-based spatial modeling of COVID-19 incidence rate in the continental United States, *Science of the Total Environment*, 1, 138884 (2020).
- [7] A. Atangana and S. I. Araz, Mathematical model of COVID-19 spread in Turkey and South Africa: theory, methods, and applications, *Advances in Difference Equations*, 1, 1-89 (2020).
- [8] A. N. Gois, E. E. Laureano, D. D. Santos, D. E. Sanchez, L. F. Souza, R. D. Vieira, J. C. Oliveira, and E. Santana-Santos, Lockdown as an intervention measure to mitigate the Spread of COVID-19: a modeling study, *Revista da Sociedade Brasileira de Medicina Tropical*, 53 (2020).
- [9] M. Makhoul, H. Chemaitelly, H. Ayoub, S. Seedat and L. J Abu-Raddad, Epidemiological differences in the impact of COVID-19 vaccination in the United States and China, *Vaccines*, 9, 223 (2021).
- [10] P. C. Jentsch, M. Anand, and C. T. Bauch, Prioritising COVID-19 vaccination in changing social and epidemiological landscapes: a mathematical modelling study, *The Lancet Infectious Diseases*, (2021).
- [11] S. Moore, E. M. Hill, M. J. Tildesley, L. Dyson, and M. J. Keeling, Vaccination and non-pharmaceutical interventions for COVID-19: a mathematical modelling study, *The Lancet Infectious Diseases*, 21, 793-802 (2021).
- [12] S. M. Moghadas, T. N. Vilches, K. Zhang, S. Nourbakhsh, P. Sah, M. C. Fitzpatrick, and A. P. Galvani, Evaluation of COVID-19 vaccination strategies with a delayed second dose, *PLoS Biology*, 19, e3001211 (2021).
- [13] A. Olivares and E. Staffetti, Uncertainty quantification of a mathematical model of COVID-19 transmission dynamics with mass vaccination strategy, *Chaos, Solitons & Fractals*, 146, 110895 (2021).
- [14] F. P. Polack, S. J. Thomas, N. Kitchin, J. Absalon, A. Gurtman, S. Lockhart, J. L. Perez, G. Perez Marc, E. D. Moreira, C. Zerbini, and R. Bailey, Safety and efficacy of the BNT162b2 mRNA Covid-19 vaccine, *New England Journal of Medicine*, 383, 2603-2615 (2020).
- [15] L. R. Baden, H. M. El Sahly, B. Essink, K. Kotloff, S. Frey, R. Novak, D. Diemert, S. A. Spector, N. Rouphael, C. B. Creech, and J. McGettigan, Efficacy and safety of the mRNA-1273 SARS-CoV-2 vaccine, *New England Journal of Medicine*, 384, 403-416 (2021).
- [16] M. Voysey, S. A. C. Clemens, S. A. Madhi, L. Y. Weckx, P. M. Folegatti, P. K. Aley, B. Angus, V. L. Baillie, S. L. Barnabas, Q. E. Bhorat, and S. Bibi, Safety and efficacy of the ChAdOx1 nCoV-19 vaccine (AZD1222) against SARS-CoV-2: an interim analysis of four randomised controlled trials in Brazil, South Africa, and the UK, *The Lancet*, 397, 99-111 (2021).
- [17] N. Dagan, N. Barda, E. Kepten, O. Miron, S. Perchik, M. A. Katz, M. A. Hernan, M. Lipsitch, R. Reis, R. D. Balicer, BNT162b2 mRNA Covid-19 vaccine in a nationwide mass vaccination setting, *New England Journal of Medicine*, 384, 1412-1423 (2021).
- [18] B. H. Foy, B. Wahl, K. Mehta, A. Shet, G. I. Menon, and C. Britto, Comparing COVID-19 vaccine allocation strategies in India: A mathematical modelling study, *International Journal of Infectious Diseases*, 103, 431-438 (2021).
- [19] The Republic of South Africa's department of Health online resource and news portal on COVID-19, <https://www.SAcoronavirus.co.za> (2021).
- [20] US Food and Drug Administration, <https://www.fda.gov> (2021).
- [21] G. N. Wong, Z. J. Weiner, A. V. Tkachenko, A. Elbanna, S. Maslov, and N. Goldenfeld, Modeling COVID-19 dynamics in Illinois under nonpharmaceutical interventions, *Physical Review X*, 10, 041033 (2020).
- [22] T. Sun and Y. Wang, Modeling COVID-19 epidemic in Heilongjiang province, China, *Chaos, Solitons and Fractals*, 138, 109949 (2020).
- [23] B. Boukanjime, T. Caraballo, M. El Fatini, and M. El Khalifi, Dynamics of a stochastic coronavirus (COVID-19) epidemic model with Markovian switching, *Chaos, Solitons and Fractals*, 141, 110361 (2020).
- [24] D. M. Kennedy, G. J. Zambrano, Y. Wang, and O. P. Neto, Modeling the effects of intervention strategies on COVID-19 transmission dynamics, *Journal of Clinical Virology*, 128, 104440 (2020).
- [25] R. N. Thompson, T. D. Hollingsworth, V. Isham, D. Arribas-Bel, B. Ashby, T. Britton, P. Challenor, L. H. Chappell, H. Clapham, N. J. Cunniffe, and A. P. Dawid, *Key questions for modelling COVID-19 exit strategies*, Proceedings of the Royal Society B, 287, 20201405 (2020).
- [26] W. Lyra, J. D. do Nascimento Jr, J. Belkhiria, L. de Almeida, P. P. Chrispim, I. de Andrade, COVID-19 pandemics modeling with modified determinist SEIR, social distancing, and age stratification. The effect of vertical confinement and release in Brazil, *Plos One*, 15, e0237627 (2020).
- [27] G. B. Libotte, F. S. Lobato, G. M. Platt, and A. J. Neto, Determination of an optimal control strategy for vaccine administration in COVID-19 pandemic treatment, *Computer Methods and Programs in Biomedicine*, 196, 105664 (2020).
- [28] S. M. Garba, J. M. Lubuma, and B. Tsanou, Modeling the transmission dynamics of the COVID-19 Pandemic in South Africa, *Mathematical Biosciences*, 328, 108441 (2020).
- [29] M. Sadarangani, B. A. Raya, J. M. Conway, S. A. Iyaniwura, R. C. Falcao, C. Colijn, D. Coombs, and Gantt, Importance of COVID-19 vaccine efficacy in older age groups, *Vaccine*, 39, 2020-2023 (2021).
- [30] K. M. Bubar, K. Reinholt, S. M. Kissle, M. Lipsitch, S. Cobey, Y. H. Grad, and D. B. Larremore, Model-informed COVID-19 vaccine prioritization strategies by age and serostatus, *Science*, 371, 916-921 (2021).
- [31] E. A. Iboi, C. N. Ngonghala, and A. B. Gumel, Will an imperfect vaccine curtail the COVID-19 pandemic in the US?, *Infectious Disease Modelling*, 5, 510-524 (2020).

- [32] M. Rabi, R. Willie, and N. Parumasur, Mathematical analysis of a disease-resistant model with imperfect vaccine, quarantine and treatment, *Ricerche di Matematica*, 69, 1-25 (2020).
- [33] H. L. Smith and P. Waltman, *The theory of the chemostat: dynamics of microbial competition*, Cambridge University Press, (1995).
- [34] S. M. Garba, M. A. Safi, and S. Usaini, Mathematical model for assessing the impact of vaccination and treatment on measles transmission dynamics, *Mathematical Methods in the Applied Sciences*, 40, 6371-6388 (2017).
- [35] C. Castillo-Chavez, B. Song, and W. Huang, On the computation of  $R_0$  and its role in global stability, *IMA Volumes in Mathematics and its Applications*, 125, 229-250, (2002).
- 



**Musyoka Kinyili** is a PhD fellow in Applied Mathematics at the University of the Western Cape. His research interests are in the areas of Statistical Signal Processing, Ordinary Differential Equations and Epidemiological Modelling.



**Justin B. Munyakazi** is an Associate Professor of Mathematics at the University of the Western Cape. His research interests span the area of Numerical Analysis, Computational Mathematics and Biomathematics.



**Abdulaziz Mukhtar** is a PhD holder and lecturer in Department of the Mathematics and Applied Mathematics at the University of the Western Cape. His research interests lie in Biomathematics and Statistical Inference.